
How Interpretable and Trustworthy are GAMs?

Chun-Hao Chang¹²³, Sarah Tan⁴, Ben Lengerich⁵, Anna Goldenberg¹²³, Rich Caruana⁶

¹University of Toronto, ²Vector Institute, ³The Hospital for Sick Children

⁴Cornell University, ⁵Carnegie Mellon University, ⁶Microsoft Research

kingsley@cs.toronto.edu, ht395@cornell.edu, blengeri@andrew.cmu.edu,

anna.goldenberg@utoronto.ca, rcaruana@microsoft.com

Abstract

Generalized additive models (GAMs) have become a leading model class for data bias discovery and model auditing. However, there are a variety of algorithms for training GAMs, and these do not always learn the same things. Statisticians originally used splines to train GAMs, but more recently GAMs are being trained with boosted decision trees. It is unclear which GAM model(s) to believe, particularly when their explanations are contradictory. In this paper, we investigate a variety of different GAM algorithms both qualitatively and quantitatively on real and simulated datasets. Our results suggest that inductive bias plays a crucial role in model explanations and tree-based GAMs are to be recommended for the kinds of problems and dataset sizes we worked with.

1 Introduction

As the impact of machine learning on our daily lives continues to grow, we have begun to require that ML systems used for high-stakes decisions (e.g., healthcare or criminal justice) not only be accurate, but also satisfy other properties such as fairness or interpretability [4, 11]. Generalized additive models (GAMs) have emerged as a leading model class that is designed to be simple enough for human to simulate how it works yet remains accurate. In one well-known example, Caruana et al. [2] showed that GAMs helped uncover a counter-intuitive pattern in a pneumonia dataset that asthma lowers the risk of dying from pneumonia. Tan et al. [20] also use GAMs to audit black-box models to check if they are biased against minority groups.

GAMs were originally fit using smoothing splines [6], but more recently are being fit with tree-based methods [2] or fused LASSO additive models [21]. This paper shows that different GAMs can have similar accuracy and make highly-correlated predictions, yet their explanations can be very different. To see how important this can be, imagine a model which shows no effect on variables such as race or gender, and thus appears to be unbiased, but which has compiled the bias into other correlated variables that are less obviously related to race and gender, allowing the bias to go unrecognized. In this paper we investigate which GAMs tend to model predictions using fewer, correlated features (thus potentially hiding bias), and which GAMs spread signal more uniformly among many variables.

Even when a GAM does not hide bias, does it faithfully characterize patterns that are in the data? A more complex GAM might be less likely to hide bias, but also be more likely to learn spurious patterns that do not generalize to unseen instances. Yet overly simple GAMs such as linear regression will not be able to capture non-linear relationships in the data and thus will fail to show the full story. To address these issues, we empirically compare various GAMs on a wide variety of both real-world and simulated datasets. Our key contributions can be summarized as follows:

- We compare different GAM algorithms on 10 classification datasets and find that the most accurate GAM methods yield similar accuracy, yet learn qualitatively different explanations.

- We measure the impact of GAMs that make predictions using many features (similar to ℓ_2 -regularized model), and those that use few features (ℓ_1 regularization), on the resulting explanations.
- We analyze the bias-variance tradeoff between GAMs: if two GAMs have similar accuracy, explanations from low bias, high variance GAMs are more trustworthy [19] than explanations from high bias, low variance GAMs.
- We compare models on semi-simulated datasets where we know the ground truth explanations, and find that tree-based GAMs have the best worst-case explanation error of the different GAM types.
- The empirical evidence suggests that inductive bias plays a crucial role in model explanations, and we recommend tree-based GAMs over other GAMs for problems like the ones we considered.

2 GAM models

Generalized additive models (GAMs) can be expressed as follows. Given an input $x \in \mathbb{R}^{N \times D}$, a label y , a link function g and shape functions f_j for each feature a GAM has the form

$$g(y) = f_0 + \sum_{j=1}^D f_j(x_j).$$

GAMs are interpretable because the impact of each f_j can be visualized as a graph, and human can easily simulate how a GAM works by reading f_j from the graph and add them together.

Explainable Boosting Machine (EBM): a type of GAM designed to provide both intelligibility and high accuracy [12, 2, 14]. In EBMs, shape functions are gradient-boosted ensembles of bagged trees, each tree operating on a single variable. Trees are estimated in a round-robin manner which forces the model to sequentially consider each variable as an explanation of the current residual rather than greedily selecting the best feature. This construction spreads influence among correlated variables, and has been used to uncover meaningful and unexpected effects in healthcare data [2]. For comparison, we create a variation of EBM — EBM-BF (EBM-BestFirst) — that greedily split the best feature to reduce error at each iteration, similar to traditional gradient boosted trees.

Figure 1(a) shows graphs for four shape functions trained on the MIMIC-II dataset using EBM and EBM-BF. The first three features are continuous (Age, PFRatio, and Systolic Blood Pressure (SBP)), and the fourth is boolean (AIDS). In the shape plots higher scores (up) indicate higher ICU mortality risk and vice versa. The graph of risk as a function of age suggests that risk is reasonably low until age 50, then begins to rise rapidly, levels off for patients age 90-105, then rises again past 105. Both EBM and EBM-BF learn similar risk profiles for Age, PFRatio and SBP.

For AIDS, however, the models are qualitatively different: EBM has learned that AIDS lowers risk, while EBM-BF predicts that AIDS neither increases nor decreases risk (Fig. 1(a), top right corner). One possible reason is since EBM-BF train trees on the best next feature, it tends to put more weight on important features (more ℓ_1) and thus ignore weaker features like AIDS.

XGBoost: we introduce a new tree-based GAM based on the popular boosting package XGBoost [3]. XGBoost uses second order derivatives and regularization to achieve better performance. To convert XGB to a GAM, we limit tree depth to 1 (stumps) so trees are not able to learn feature interactions, and bag XGB 100 times to improve accuracy (similar to EBM). We also create a new version of XGB, "XGB-L2", similar to EBMs, that picks features randomly when growing trees instead of choosing the best features greedily: we set the XGB random subsampling of features parameter to a small ratio such that each tree is given just 1 feature. This modification makes XGB more of an " ℓ_2 "-type model, that will use all features. Figure 1(b) show these 2 methods. Shape plots learned by XGB, XGB-L2 and EBM tend to agree with each other in large-sample regions, but diverge in low-sample regions on Age, PFRatio and SBP.

Splines: GAMs were first fit using smoothing splines [6]. We tried a variety of spline methods in 2 packages, pygam [18] and R mgcv package [22]. Cubic splines in pygam appear to have a good combination of accuracy and robustness and is used for all of our experiments. We set the number of basis functions to 50 for all datasets.

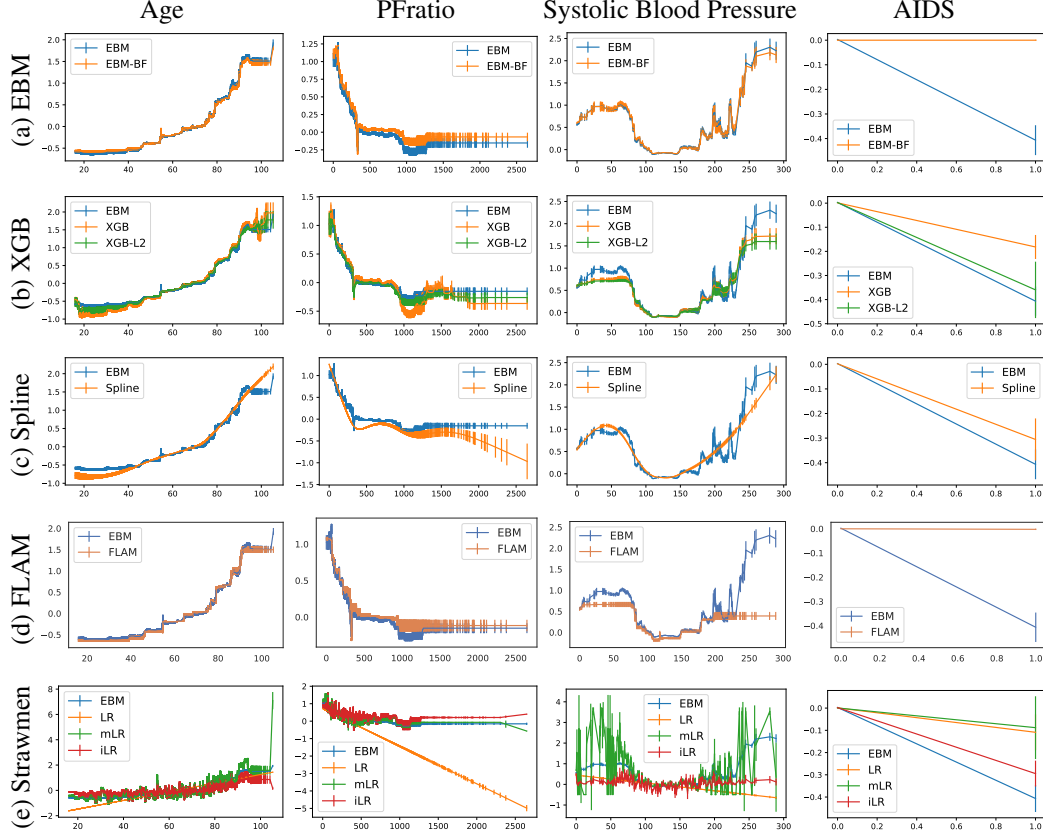


Figure 1: The shape plots of total 9 intelligible GAM models trained on the MIMIC-II dataset (shape plots for 4 of the 17 features shown). We repeat EBM (blue) in each plot for comparisons.

In Figure 1(c), we see that the spline shape functions for Age, PFratio and SBP are much smoother compared to tree-based methods such as EBM and XGB. Although this smoothness does not hurt accuracy much, it has significant effects on the shape plots. For example, splines do not capture the drop in risk that happens in the PFratio plots at 332. PFratio is a measure of how effectively patients convert O_2 in the air to O_2 in their blood. This drop in risk at 332 is due to missing PF values being imputed with the mean value of this feature: because PFratio is not measured for patients who are believed to have healthy O_2 respiration, it is often missing for healthier patients, and when imputed with the mean we see a drop in risk corresponding to this group of healthier patients right at the mean value of the feature. The spline is thus distorted in the region 300-600 because of this strong effect of the sharp drop in risk near PFratio = 332.

Splines also completely miss the jumps in the SBP graphs that occur at 175, 200 and 225 trained by EBM and XGB: these jumps and dips in risk are due to treatment effects, since 175, 200, and 225 are treatment thresholds doctors use. As the patient's SBP rise and reach the threshold, risk actually drops because most patients just above the threshold receive more aggressive treatment that is effective at reducing their risk.

Fused LASSO Additive Models (FLAM) For each unique value of feature x_j , Fused LASSO Additive Model (FLAM) learns a weight on each value, and adds ℓ_1 penalty on the adjacent weights differences. Due to the sparsity of ℓ_1 , FLAM produces relatively flat graph and penalizes unnecessary jumps. We use the R package FLAM [15]. In Figure 1(d), we show FLAM model is more similar to tree-based models but flatter and thus misses some patterns. For example in SBP graph, FLAM appears to miss the treatment effects in the SBP graph but found by EBM and XGB for SBP near 175, 200 and 225. FLAM also shows (similar to EBM-BF) that AIDS has no effect on the target.

Logistic regression (LR) and other strawman approaches We compare our approaches to Logistic Regression (LR), a widely used linear model that cannot learn non-linear shape plots. We also compare to two other strawmen: marginalized LR (**mLR**) and indicator LR (**iLR**). We first bin each feature x_j into at most 255 bins. Instead of LR which assumes the $f_j(x_j) = w_j x_j$, **mLR** sets $f_j(x_j) = w_j g(x_j)$ where $g(x_j)$ is the average (marginalized) value of target y within the same bin as x_j in the dataset. **iLR** treats each bin as a new feature (similar to one-hot encoding) and learns an LR on top of it. It ignores the proximity relationship across the feature values. As expected, the shape plots for LR are straight lines that miss much of the interesting detail in the data. Despite this, LR has reasonably competitive accuracy in Table 1. iLR and mLR, however, are even less accurate than LR. iLR appears to be too heavily regularized to learn the details in the MIMIC-II data, and mLR appears to not be regularized enough and shows high noise in Figure 1(e).

Organization We will start by comparing GAM training algorithms qualitatively (Sec. 3.1) and quantitatively in terms of predictive accuracy (Sec. 3.2). We then inspect how different GAMs spread the influence of features more widely or narrowly (Sec. 3.3), and do bias-variance analysis (sec. 3.4). Section 4 focuses on simulated datasets which we know the ground-truth explanations (shape graphs), and we measure the explanation error (sec. 4.1) and how correlated it is to the predictive performance (sec. 4.2). Finally we mention the related work (Sec. 5) and conclusion (Sec. 6). We describe training details and hyperparameters in Appendix A, and more experiments and shape graphs in Appendix B.

3 Real datasets

3.1 COMPAS: an example where different GAMs reveal different biases

Here we present a case study of the COMPAS recidivism dataset. Figure 2 presents the shape functions of five GAM algorithms – EBM, XGB, Spline, FLAM and LR – trained on this dataset. The first four GAM methods (i.e. excluding LR) have no substantial difference in AUC (Table 1). However, we observe in Figure 2a (Race) that all five methods have the same sign for each race, but with varying magnitudes. The biggest disagreement happens for Asian race: FLAM and XGB have small magnitude while others have large magnitude. In Figure 2b (Age) graph, all the methods agree between age 20 to 70 with decreasing risk, but have very different estimates over age 70. Both EBM and XGB have an interesting increase from 75 to 80, and remain flat after. Spline, on the other hand, says the risk slowly increases after 70s. FLAM indicates no risk difference after 55, and LR says the risk keeps decreasing due to its linear nature. In Figure 2c (length of stay), both EBM and XGB have two interesting dips around 150 (1/2 year) and 270 (3/4 year). Then they have an abrupt increase between 300 to 350, and remain flat afterward. Spline vaguely agrees with EBM and XGB by having smaller risk between 100 and 300, but keeps extrapolating to an extremely high risk of 10, probably due to the small sample size in the far right region and its smoothing prior. FLAM surprisingly mostly remains flat (no risk difference), and LR increases the risk slowly and linearly. Similar patterns can be observed in Figure 2d (priors counts).

Overall, EBM and XGB have interesting dips and jumps that may give clues to the underlying data patterns. Spline tends to extrapolate over-confidently in the low-sample regions. FLAM gives relatively simple and flat explanations. Lastly, LR is the simplest approach but is unable to recover anything beyond linear patterns, limiting its use for data bias discovery. In the following sections, we quantitatively compare which GAM is more trustworthy and hides the bias less.

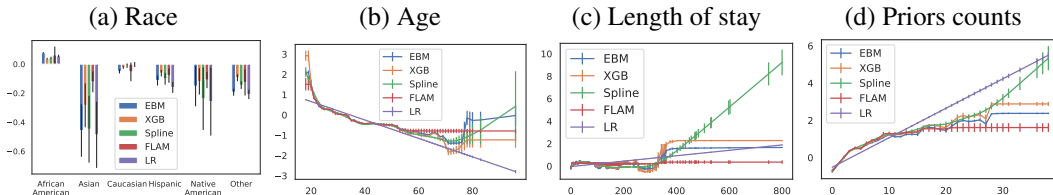


Figure 2: GAM’s shape plots of COMPAS dataset (Race, Age, Length of Stay, and Priors counts).

Table 1: Test set AUCs across 10 datasets. Best number in each row in **bold**.

	GAM									Full Complexity	
	EBM	EBM-BF	XGB	XGB-L2	FLAM	Spline	iLR	LR	mLR	RF	XGB-d3
Adult	0.930	0.928	0.928	0.917	0.925	0.920	0.927	0.909	0.925	0.912	0.930
Breast	0.997	0.995	0.997	0.997	0.998	0.989	0.981	0.997	0.985	0.993	0.993
Churn	0.844	0.840	0.843	0.843	0.842	0.844	0.834	0.843	0.827	0.821	0.843
Compas	0.743	0.745	0.745	0.743	0.742	0.743	0.735	0.727	0.722	0.674	0.745
Credit	0.980	0.973	0.980	0.981	0.969	0.982	0.956	0.964	0.940	0.962	0.973
Heart	0.855	0.838	0.853	0.858	0.856	0.867	0.859	0.869	0.744	0.854	0.843
MIMIC-II	0.834	0.833	0.835	0.834	0.834	0.828	0.811	0.793	0.816	0.860	0.847
MIMIC-III	0.812	0.807	0.815	0.815	0.812	0.814	0.774	0.785	0.776	0.807	0.820
Pneumonia	0.853	0.847	0.850	0.850	0.853	0.852	0.843	0.837	0.845	0.845	0.848
Support2	0.813	0.812	0.814	0.812	0.812	0.812	0.800	0.803	0.772	0.824	0.820
Average	0.866	0.862	0.866	0.865	0.864	0.865	0.852	0.853	0.835	0.855	0.866
Rank	3.70	6.70	3.40	4.90	5.05	4.60	8.70	7.75	9.70	7.40	4.10
Score	0.893	0.781	0.873	0.818	0.836	0.810	0.474	0.507	0.285	0.543	0.865

3.2 Which GAM has the best generalization in real datasets?

Table 1 provides test set AUC for 10 datasets from different domains, with varying sizes ($100s - 10^5s$), and number of features (6 - 57) (see Table 5 for details). Besides the 9 GAM algorithms described in Section 2, we also include 2 full-complexity methods: Random Forest (RF) and XGB with depth 3 (XGB-d3). Each dataset was randomly split into 70-15-15% train-val-test splits and run for 5 times. See Table 11 for results with standard deviation. To consider the results in aggregate for each method, we compute three metrics for each method: (1) Average test AUC over 10 datasets; (2) Rank: rank each method’s performance compared to other methods on each dataset, then average ranks over all 10 datasets (the lower the rank the better). (3) Normalized score on each dataset: for each dataset, set the lowest test AUC for that dataset as 0 and the highest as 1, and scale all other scores linearly between 0 and 1. Among GAM methods, EBM and XGB perform the best, with XGB-L2, Spline and FLAM very close. EBM-BF comes in the fifth place with 3 baselines, iLR, LR and mLR, performing the worst. For full complexity methods, XGB-d3 is much better on average than RF, but performs slightly worse than EBM and XGB on two other metrics Rank and Score. Within the 10 datasets we profile, GAM model is on par with full complexity methods, while still remaining interpretable.

3.3 Which GAM makes predictions using multiple features (ℓ_2 -ish) or just a few (ℓ_1 -ish)?

Consider a data set where there is significant correlation among features (which is very common). A model using a few features (ℓ_1 -ness) will have used the correlation to “compile” the effect of weaker features into the stronger features, allowing it to place little or no learned effect on the weak ones. It makes users unaware of such effect exists. In contrast, an ℓ_2 -ness model will show potentially

Table 2: ℓ_2 -ness Metrics. The higher the number, the more features the model uses.

	EBM	EBM-BF	XGB-L2	XGB	LR	LASSO	FLAM	Spline
Adult	0.271	0.226	0.339	0.290	0.220	0.213	0.211	0.205
Breast	0.086	0.059	0.112	0.070	0.130	0.066	0.077	0.234
Churn	0.157	0.130	0.150	0.129	0.199	0.162	0.131	0.227
Compas	0.183	0.170	0.183	0.179	0.177	0.177	0.172	0.173
Credit	0.269	0.158	0.269	0.194	0.124	0.122	0.170	0.191
Heart	0.240	0.218	0.287	0.250	0.326	0.308	0.215	0.154
MIMIC-II	0.204	0.186	0.205	0.196	0.194	0.194	0.188	0.210
MIMIC-III	0.207	0.148	0.212	0.187	0.190	0.187	0.186	0.216
Pneumonia	0.297	0.206	0.299	0.253	0.272	0.258	0.258	0.195
Support2	0.124	0.117	0.114	0.130	0.103	0.102	0.114	0.126
Average	0.204	0.162	0.217	0.188	0.194	0.179	0.172	0.193

interesting effects on all or most of the features, allowing human to have a final say of whether or not to believe the patterns. Therefore we argue ℓ_2 -ness model is more favorable in data bias discovery.

We design a metric to quantify the ℓ_1 -ness versus ℓ_2 -ness. For each GAM, we greedily add the most important features to it, one at a time, and see how model reduces its test set error. As a result, the faster the model's error reduces, the fewer features it depends on. For each method, we scale its initial error as 1 and the final error as 0. We then measure the area under the curve for each method.

We show two examples, Adult and Breast, in supplementary Figure 7, and show the quantitative results in Table 2. First, as we expect it, EBM is consistently having higher ℓ_2 -ness metrics than EBM-BF, as it uses more features just by design. Similarly, XGB-L2 also has higher metric than XGB. Compared to EBM, XGB is consistently having higher ℓ_2 -ness than its corresponding variant (XGB to EBM-BF, and XGB-L2 to EBM). LR is also consistently higher than LASSO. FLAM is also a very ℓ_1 -ish method as it tends to penalize out unused features, and is consistently smaller than XGB. Finally, Spline does not have a pattern, as it fluctuates quite a bit from dataset to dataset. For example, Spline gets the smallest for the Adult dataset but having largest ℓ_2 -ness in the Breast dataset. To summarize, EBM and XGB-L2 has higher ℓ_2 -ness and thus do not tend to hide the effect from user.

3.4 Which GAM has lower bias and thus recover data patterns more faithfully?

We now do a bias-variance analysis. In bias-variance analysis, bias is the result of misspecifying the model to underlying data patterns, and variance is the complexity of the model [7]. In explanatory modeling the focus is on minimizing bias to obtain the most accurate representation of the underlying data patterns, but not variance [19]. Thus if two models have similar accuracy, we should trust explanations from models with low bias as their explanation is closer to the ground truth.

To measure bias and variance, we follow the procedure of Munson and Caruana [13]. For each round, we split our dataset into 15% for test set and 85% for training set. Then we randomly subsample the training data to only 50% for 5 times and calculate bias and variance. Then we run 8 rounds and average the results.

To compare the ranking between each method, for each dataset, we take the ranking for bias and variance (detailed table in Sec. B.1), then we take the average rank across 10 datasets and plot the Figure 3 for each GAM. Here the lower rank is better (smaller). Within the top 5 methods that's closer to the left bottom corner, XGB has the lowest bias, and thus should be the most trustworthy. EBM, Spline and XGB-L2 are somewhere in the middle, with EBM-BF in the high-bias, low-variance region. Thus shape graphs from EBM-BF should be less trusted especially when EBM-BF does not have higher accuracy than others. FLAM also has lower bias and higher variance, but is not as good as XGB in both terms. To sum up, XGB has the most trustworthy explanations with smallest bias.

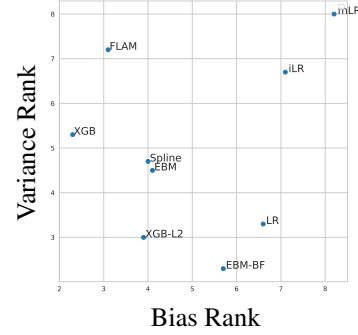


Figure 3: The average rank of bias (x-axis) vs. variance (y-axis) for each GAM across the datasets. Lower rank is better.

4 Semi-synthetic datasets

To compare the interpretability of different GAMs, we simulate datasets with ground truth shape plots. To preserve the character of real-world datasets as much as possible, we keep the data X but change the label y : first we learn multiple ground truth GAM models (EBM, XGB, Spline, FLAM and LR) on the datasets and then re-generate the label y from these models' predictions. Since these GAM models, except LR, are one of the best predicting models we can get on these datasets (Table 1), the generated labels capture the real-world distribution as close as possible. Thus we name these datasets as "semi-synthetic" datasets, to explicitly separate from the unreal synthetic datasets.

Figure 4 shows different GAMs alongside ground truth patterns from two very different generators, Spline and FLAM, on MIMIC-II for one continuous feature (PFRatio) and one boolean (AIDS). *generator bias* is clear: a method fits the ground truth best when generated by the same algorithm. For example, spline almost perfectly fits its own generator (Fig. 4(a)(c)), while doing poorly when ground truth is FLAM (Fig. 4(b)(d)), and vice versa for FLAM. Also, in PFRatio with spline generator

Table 3: The normalized graph fidelity score in the worst case scenario among 5 different generators (EBM, XGB, FLAM, Spline and LR) in the semi-synthetic datasets. The higher the better.

	EBM	EBM-BF	XGB	FLAM	Spline	LR	iLR	mLR
Breast	0.000	0.212	0.303	0.229	0.133	0.425	0.000	0.000
Churn	0.135	0.013	0.105	0.203	0.000	0.000	0.160	0.000
Heart	0.687	0.248	0.682	0.869	0.697	0.524	0.646	0.000
MIMIC-II	0.612	0.526	0.739	0.629	0.727	0.000	0.066	0.000
MIMIC-III	0.453	0.370	0.701	0.652	0.512	0.270	0.000	0.000
Pneumonia	0.400	0.000	0.602	0.644	0.036	0.000	0.268	0.064
Average	0.381	0.228	0.522	0.538	0.351	0.203	0.190	0.011

(Fig. 4(a)), tree-based methods still learn abrupt jumps at 210 even when the underlying ground truth (orange) is smooth; similarly there is also a drop at 75. This illustrates that model inductive bias is substantially affecting the resulting explanations irrespective of the true data generating patterns.

4.1 Which GAMs in the worst case have highest explanation fidelity?

To avoid the generator bias that tends to favor its own method, we instead analyze the GAM in the worst case scenario. That is, what is the worst performance each method would get out of all the different generators? As in the real world, we do not know in advance what the underlying generator is, as it could be linear, smooth or jumpy graph. To measure the explanation fidelity with respect to the ground truth generators, we measure the mean absolute difference with respect to the ground truth for each graph, and sum the error weighted by number of examples. This measures how good a method recovers the generator. Note that this is different from test set error, as one method could have a very high infidelity of the graph, but with correlated features it can still retains high test set accuracy. Since for each generator the difficulty might be different, we linearly scale the error between 0 to 1 with the worst method as 0 and the best method as 1. We refer it as normalized graph fidelity score.

In Table 3, we show the worst score for each method under 5 generators for 6 datasets. On average FLAM and XGB perform the best, with EBM and Spline coming as the third and fourth place. EBM-BF, LR, and two straemans are the least. To understand how each method makes mistakes, we further decompose this error into underestimation and overestimation error. Underestimation happens when the model estimates lower risk than the ground truth in the absolute value, while overestimation occurs when model indicates higher risk than ground truth. Then we quantitatively show the results in supplementary Table 9 and 10. We find Spline tends to quantitatively overestimate the graphs probably because it has overshooting estimates in the low-sample regions. And EBM-BF underestimates the effects too much due to its ℓ_1 -ish nature of ignoring other weak features. In summary, FLAM and XGB are the two best methods in the worst case having highest explanation fidelity. It is worth noting that this finding matches the bias-variance analysis (Sec. 3.4) that the two best methods of graph fidelity, XGB and FLAM, also have the smallest bias in real data.

4.2 Does good generalization error indicate good explanation fidelity?

To investigate how correlated of generalization error versus graph fidelity for each method, we scatter plot the ranking of the test AUC versus the ranking of graph fidelity on all 30 semi-synthetic datasets in Figure 5. If a model has high test AUC but low graph fidelity (upper left corner), then this test AUC could be misleading to the users to put more trust on its generated graphs. In Figure 5,

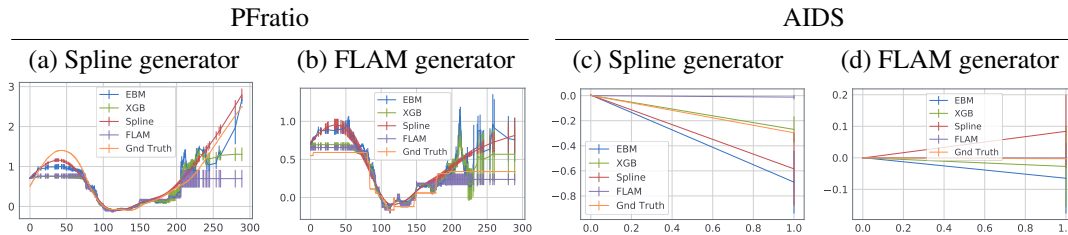


Figure 4: PFratio and AIDS graph when learning on two different generators: Spline and FLAM.

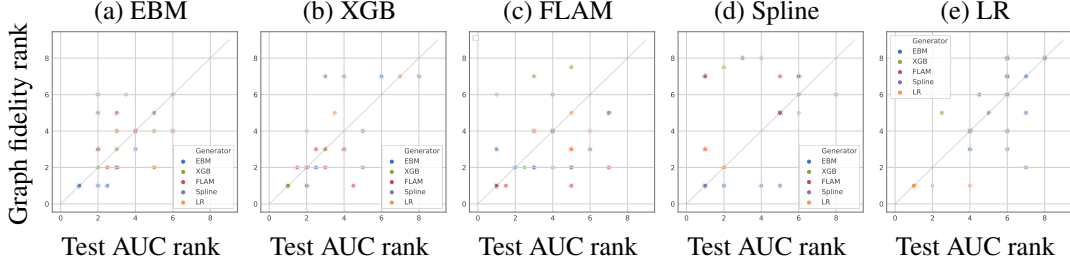


Figure 5: Scatter plot between the ranking of test AUC (x-axis) vs the ranking of graph fidelity (y-axis) for (a) EBM, (b) XGB, (c) FLAM, (d) Spline and (e) LR. Color specifies different generators, and density the number of points. Lower rank is better. The more points in the upper left corner (great AUC but terrible graph fidelity), the more unreliable of using high accuracy to indicate good fidelity.

Table 4: Summary of the key findings.

	EBM	XGB	FLAM	Spline	LR
Test acc	High	High	High	High	Low
ℓ_2 -ness	High	Med	Low	Varied	Med
Bias/Var	Med/Med	Low/High	Low/High	Med/Med	High/Low
Explanation fidelity	Med	High	High	Med	Low
Correlation to test acc.	Med	High	Low	Low	High
Qualitative	Jumpy; Easy to find patterns	Similar to EBM	Sparse and flat	Bad Extrapolation? Often too smooth.	Often too simple

XGB (b) and LR (e) are two best methods with fewer points closer to the upper left corner, with EBM in the third place. FLAM and Spline are the two worst methods with points closer to the corner. Intuitively, methods tend to have the largest discrepancy when the generator has very different inductive bias. Indeed, FLAM (Figure 5(c)) does the worst on LR generator (orange) when it gets rank 1 in test AUC while having rank 6 in graph fidelity. Similarly, Spline (Figure 5(d)) is the worst when generators are FLAM, XGB and EBM. To summarize, the high test AUC of XGB and LR imply faithful explanations, while FLAM and Spline can have high test AUC but misleading graphs.

5 Related Work

Our paper is not the first to compare different GAM algorithms, but to the best of our knowledge it is the first to focus on interpretability and systematically study differences in shape plots learned by various algorithms. Binder and Tutz [1] compared GAM algorithms, including backfitting, joint optimization, and boosting, finding that boosting performed particularly well in high-dimensional settings. Lou et al. [12] also found that boosting shallow bagged trees on each feature yielded higher accuracy than other GAM algorithms. Both papers focused on accuracy, not interpretability.

We briefly mention several other GAM methods and implementations that we did not benchmark in this paper. The `mboost` package [8] trains GAMs via boosting with several options for nonparametric smoothers. Besides splines and trees, other functional forms have been proposed to model the terms in GAMs, such as wavelets [17], trend filters [16], etc., all of which have their own inductive biases.

6 Conclusion

We summarize our key findings in Table 6. Although most accurate GAMs have very similar test accuracy, tree-based algorithm is superior operating in the data regime we consider. They not only have higher ℓ_2 -ness than FLAM and Spline, but also recover the data patterns more truthfully with lower bias in real datasets, and more stable under the worst-case scenarios in the semi-synthetic datasets. We also find tree-based algorithms having better correlation between the test accuracy and the data fidelity, making them useful when doing model selection based on the test accuracy. Qualitatively, Spline also fails to capture PFRatio (Figure 1(c)) is mean-imputed, which is easily detected by EBM, XGB and FLAM, and extrapolate over-confidently in low-sample regions (Figure 2(c)).

Within tree-based methods, EBM’s higher ℓ_2 -ness makes it easier to discover bias hidden in the data. Yet XGB is, on average, more faithful to data patterns in both real and semi-synthetic datasets. We believe our work is an important step towards making GAMs more trustworthy, and our evaluation framework will promote the development of better GAMs in the future.

Broader Impact

As interpretable models are increasingly being motivated as a tool that can be used to debug machine learning models or audit datasets, particularly to detect biases and unfairness towards certain sub-groups, it is crucial that these tools not be misleading. We demonstrated our work on a variety of datasets in the domains of criminal justice, medicine, and financial lending. Our work sheds light on how different GAM algorithms could lead to different claims of biases in these datasets. We hope that our work motivates practitioners to carefully select the best training algorithm for their dataset when using GAMs, or interpretable models more generally, to detect bias and debug models.

Acknowledgments and Disclosure of Funding

This work was created during an internship at Microsoft Research. Resources used in preparing this research were provided, in part, by the Province of Ontario, the Government of Canada through CIFAR, and companies sponsoring the Vector Institute www.vectorinstitute.ai/#partners.

References

- [1] Harald Binder and Gerhard Tutz. 2008. A comparison of methods for the fitting of generalized additive models. *Statistics and Computing* 18, 1 (2008), 87–99.
- [2] Rich Caruana, Yin Lou, Johannes Gehrke, Paul Koch, Marc Sturm, and Noemie Elhadad. 2015. Intelligible models for healthcare: Predicting pneumonia risk and hospital 30-day readmission. In *Proceedings of the 21th ACM SIGKDD international conference on knowledge discovery and data mining*. 1721–1730.
- [3] Tianqi Chen and Carlos Guestrin. 2016. XGBoost: A Scalable Tree Boosting System. In *Proceedings of the 22nd ACM SIGKDD International Conference on Knowledge Discovery and Data Mining (KDD ’16)*. ACM, New York, NY, USA, 785–794. <https://doi.org/10.1145/2939672.2939785>
- [4] Finale Doshi-Velez and Been Kim. 2017. Towards a rigorous science of interpretable machine learning. *arXiv preprint arXiv:1702.08608* (2017).
- [5] Dheeru Dua and Casey Graff. 2017. UCI Machine Learning Repository. <http://archive.ics.uci.edu/ml>
- [6] Trevor Hastie and Rob Tibshirani. 1990. *Generalized Additive Models*. Chapman and Hall/CRC.
- [7] Trevor Hastie, Robert Tibshirani, and Jerome Friedman. 2009. *The elements of statistical learning: data mining, inference, and prediction*. Springer Science & Business Media.
- [8] Torsten Hothorn, Peter Buehlmann, Thomas Kneib, Matthias Schmid, and Benjamin Hofner. 2018. *mboost: Model-Based Boosting*. <https://CRAN.R-project.org/package=mboost> R package version 2.9-1.
- [9] Alistair EW Johnson, Tom J Pollard, Lu Shen, H Lehman Li-wei, Mengling Feng, Mohammad Ghassemi, Benjamin Moody, Peter Szolovits, Leo Anthony Celi, and Roger G Mark. 2016. MIMIC-III, a freely accessible critical care database. *Scientific data* 3 (2016), 160035.
- [10] Ron Kohavi. [n.d.]. Scaling up the accuracy of naive-bayes classifiers: A decision-tree hybrid.
- [11] Zachary C Lipton. 2018. The mythos of model interpretability. *Queue* 16, 3 (2018), 31–57.

- [12] Yin Lou, Rich Caruana, and Johannes Gehrke. 2012. Intelligible Models for Classification and Regression. In *Proceedings of the 18th ACM SIGKDD International Conference on Knowledge Discovery and Data Mining (KDD '12)*. Association for Computing Machinery, New York, NY, USA, 150–158. <https://doi.org/10.1145/2339530.2339556>
- [13] M Arthur Munson and Rich Caruana. 2009. On feature selection, bias-variance, and bagging. In *Joint European Conference on Machine Learning and Knowledge Discovery in Databases*. Springer, 144–159.
- [14] Harsha Nori, Samuel Jenkins, Paul Koch, and Rich Caruana. 2019. InterpretML: A Unified Framework for Machine Learning Interpretability. *arXiv preprint arXiv:1909.09223* (2019).
- [15] Ashley Petersen, Daniela Witten, and Noah Simon. 2016. Fused lasso additive model. *Journal of Computational and Graphical Statistics* 25, 4 (2016), 1005–1025.
- [16] Veeranjanyulu Sadhanala and Ryan J Tibshirani. 2017. Additive models with trend filtering. *arXiv preprint arXiv:1702.05037* (2017).
- [17] Sylvain Sardy and Paul Tseng. 2004. AMlet, RAMlet, and GAMlet: automatic nonlinear fitting of additive models, robust and generalized, with wavelets. *Journal of Computational and Graphical Statistics* 13, 2 (2004), 283–309.
- [18] Daniel Servén and Charlie Brummitt. 2018. pyGAM: Generalized Additive Models in Python. <https://doi.org/10.5281/zenodo.1208723>
- [19] Galit Shmueli et al. 2010. To explain or to predict? *Statistical science* 25, 3 (2010), 289–310.
- [20] Sarah Tan, Rich Caruana, Giles Hooker, and Yin Lou. 2018. Distill-and-compare: Auditing black-box models using transparent model distillation. In *Proceedings of the 2018 AAAI/ACM Conference on AI, Ethics, and Society*. 303–310.
- [21] Robert Tibshirani, Michael Saunders, Saharon Rosset, Ji Zhu, and Keith Knight. 2005. Sparsity and smoothness via the fused lasso. *Journal of the Royal Statistical Society: Series B (Statistical Methodology)* 67, 1 (2005), 91–108.
- [22] S. N. Wood. 2011. Fast stable restricted maximum likelihood and marginal likelihood estimation of semiparametric generalized linear models. *Journal of the Royal Statistical Society (B)* 73, 1 (2011), 3–36.
- [23] Marvin N Wright and Inke R König. 2019. Splitting on categorical predictors in random forests. *PeerJ* 7 (2019), e6339.

A Datasets, Hyperparameters and training details

We provide the code anonymous here¹.

A.1 Dataset descriptions

We list our datasets details in Table 5 and list the sources here:

- Adult dataset [10]: <https://archive.ics.uci.edu/ml/machine-learning-databases/adult/adult.data>
- Breast cancer dataset (from UCI [5])
- Credit dataset: <https://www.kaggle.com/mlg-ulb/creditcardfraud>
- Churn: <https://www.kaggle.com/blastchar/telco-customer-churn>
- COMPAS dataset is obtained from <https://www.kaggle.com/danofer/compass>.
- Heart disease dataset (from UCI [5]) <https://archive.ics.uci.edu/ml/datasets/Heart+Disease>
- MIMIC-II and MIMIC-III dataset [9]
- For Pneumonia dataset, we thank the authors of Caruana et al. [2] to run the code for us on their data server.
- Support2 dataset obtained from <http://biostat.mc.vanderbilt.edu/DataSets>

Table 5: Dataset statistics and descriptions.

	Domain	N	P	Positive rate	Description
Adult	Finance	32,561	14	24.08%	Income prediction
Breast Cancer	Medicine	569	30	62.74%	Cancer classificaiton
Churning	Finance	7,043	19	26.54%	Subscription churner
Credit	Finance	284,807	30	0.17%	Fraud detection
COMPAS	Law	6,172	6	45.51%	Reoffense risk scores
Heart	Medicine	457	11	45.95%	Heart Disease
MIMIC-II	Medicine	24,508	17	12.25%	ICU mortality
MIMIC-III	Medicine	27,348	57	9.84%	ICU mortality
Pneumonia	Medicine	14,199	46	10.86%	Mortality
Support2	Medicine	9,105	29	25.92%	Hospital mortality

A.2 Model hyperparameters and training details

Here we describe the training details for each model. We set the hyperparameters as the best for each model:

- EBM, EBM-BF: we use the open-source package from here <https://github.com/interpretml/interpret>. We set the parameters inner bagging as 100 and outer bagging as 100; improving number of bagging does not further improve performance. We use the default learning rate 0.01, default stopping patience set to 50 and 20000 episodes to make sure it converges.
- XGB, XGB-d3, XGB-L2: we use the open source package here <https://xgboost.readthedocs.io/en/latest/index.html>. We also use default learning rate with the same early stopping patience set as 50 and number of trees as maximum 30,000. We use bagging of 100 times and depth 1 for our XGB GAM model. For XGB-d3 (XGB with tree depth 3), we find that bagging of XGB-d3 hurts the performance a bit, and thus do not apply any bagging for XGB-d3. For XGB-L2, we set the parameter "colsample_bytree" as a small value 1e-5 to make sure each tree only sees one feature.

¹ https://drive.google.com/file/d/1VZRFJ4L1ULz_OEPgQca4gucmib9q41x6/view?usp=sharing

Table 6: The test set AUC of Label encoding (LE) v.s. Onehot encoding of the catogorical features for EBM and XGB on 6 datasets with categorical features.

	EBM-LE	EBM-Onehot	XGB-LE	XGB-Onehot
Adult	0.9301	0.9286	0.9281	0.9280
Churn	0.8437	0.8434	0.8436	0.8439
COMPAS	0.7429	0.7430	0.7439	0.7438
Diabetes	0.6701	0.6720	0.6706	0.6744
Heart	0.8568	0.8554	0.8454	0.8497
Support2	0.8127	0.8122	0.8131	0.8130
Average	0.8094	0.8091	0.8074	0.8088

- FLAM: we use the package from R <https://cran.r-project.org/web/packages/flam/flam.pdf>. We use 15% validation set to select the best λ penalty parameter in the fused LASSO, and then refit the whole data with the best penalty parameter. We set the parameter number of lambda as 100 and the minimum ratio as 1e-4 to increase the performance of the model.
- Spline: we use the pygam package [18]. We set the number of basis functions to be 50 and the maximum iteration as 500. We find increasing number of basis functions more than 50 would result in instability when fitting in large datasets.
- LR: we use scikit-learn’s LogisticRegressionCV with $Cs = 12$ (grid search for 12 different ℓ_2 penalty) and cross validation for 5 times to choose the best ℓ_2 , and re-fit on the whole data.
- iLR, mLR: we use the EBM package’s preprocessor to quantily bin the features into 255 bins. Then we use LR on top of it to train a linear model.

Couple GAM methods we try but does not include in the main results:

- SKGBT: we try the gradient boosting tree in scikit-learn also with tree depth set as 1. The result is pretty similar to EBM so we do not compare them in the paper.
- Cubic spline and plate spline in R mgcv package: to our surprise, the most popular spline package in R is really unstable in two datasets, Breast Cancer and Churn. We find that the reason is that mgcv can not handle numerical instability when the prediction is too close to 0 or 1.

A.3 Choosing input encoding for categorical features for each GAM

For datasets with categorical variables, it turns out that encoding tends to affect the both the shape graphs and the accuracy. For gradient boosting trees, one might think that using label encoding (LE) is better than one-hot encoding, as one-hot encoding has been shown to have inferior performance in ensemble trees [23]. In Table 6, we investigate the effects of two types of encoding on EBM and XGB. In 6 of the datasets with categorical features, EBM with label encoding (LE) indeed shows superior performance to one-hot encoding. However, for XGB, one-hot encoding performs slightly better on average. We also qualitatively examine one of the categorical features (Race) in the COMPAS dataset. In Figure 6, we find that EBM shape plots have similar patterns whether LE or one-hot encoding is used, but XGB with LE gives much smaller effect than one-hot encoding in the category Asian, suggesting that the order of the features affects its estimate. Thus we use LE for EBM and one-hot encoding for XGB. For the rest of the methods, we use LE for mLR and one-hot encoding for FLAM, Spline, LR and iLR as these methods can not handle inadequate numerical ordering.

B Additional experiments results

B.1 Bias and Variance ranking results for each dataset

Here we show the bias ranking for each dataset in Table 7 and variance ranking in Table 8. The lower rank means the better (smaller bias or variance). We see that on average XGB has the lowest bias ranking, and EBM-BF has the smallest variance.

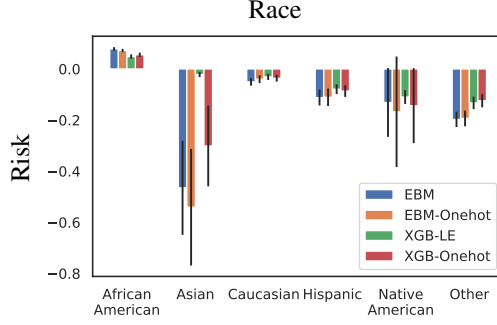


Figure 6: Label encoding (LE) v.s. Onehot encoding for EBM and XGB on the Race feature in the COMPAS dataset. For EBM, these two encodings do not make a big difference. But for XGB, XGB-LE has much smaller effect in Asian compared to XGB-Onehot, suggesting the ordering of the features from LE affects its estimate.

Table 7: Bias ranking for each dataset. The lower rank the better.

	EBM	EBM-BF	XGB	XGB-L2	FLAM	Spline	iLR	LR	mLR
Adult	1	4	3	8	6	7	2	9	5
Breast	5	6	2	4	1	7	9	3	8
Churn	4	7	1	6	2	3	8	5	9
COMPAS	6	2	1	4	5	3	7	8	9
Credit	5	7	2	4	3	1	6	9	8
Heart	4	8	3	1	5	6	7	2	9
MIMIC-II	2	6	4	3	1	5	8	7	9
MIMIC-III	5	6	3	1	2	4	9	7	8
Pneumonia	4	5	3	6	2	1	7	9	8
Support2	5	6	1	2	4	3	8	7	9
Average	4.1	5.7	2.3	3.9	3.1	4	7.1	6.6	8.2

Table 8: Variance ranking for each dataset. The lower rank the better.

	EBM	EBM-BF	XGB	XGB-L2	FLAM	Spline	iLR	LR	mLR
Adult	5	2	3	1	7	8	9	4	6
Breast	8	5	4	3	9	6	1	7	2
Churn	3	4	6	1	8	5	7	2	9
COMPAS	5	2	6	4	7	3	8	1	9
Credit	5	1	2	3	6	7	8	4	9
Heart	3	2	8	4	6	1	5	7	9
MIMIC-II	5	3	6	4	7	2	8	1	9
MIMIC-III	3	2	6	4	7	5	8	1	9
Pneumonia	3	1	6	2	8	7	5	4	9
Support2	5	1	6	4	7	3	8	2	9
Average	4.5	2.3	5.3	3	7.2	4.7	6.7	3.3	8

B.2 ℓ_2 -ness example figures

Here we show two examples, Adult and Breast, in Figure 7. We normalize the test error between 0 and 1 and measure the area under the curve as the ℓ_2 -ness. The faster it decays, the smaller the area is and the less GAM depends on multiple features.

B.3 The overestimation error and underestimation table

Here we show the results of measuring the overestimation error or underestimation error in Table 9 and 10. Here the higher score means the less error. The EBM-BF has the least overestimation error (highest score) and highest underestimation error (lowest score), probably due to its ℓ_1 nature

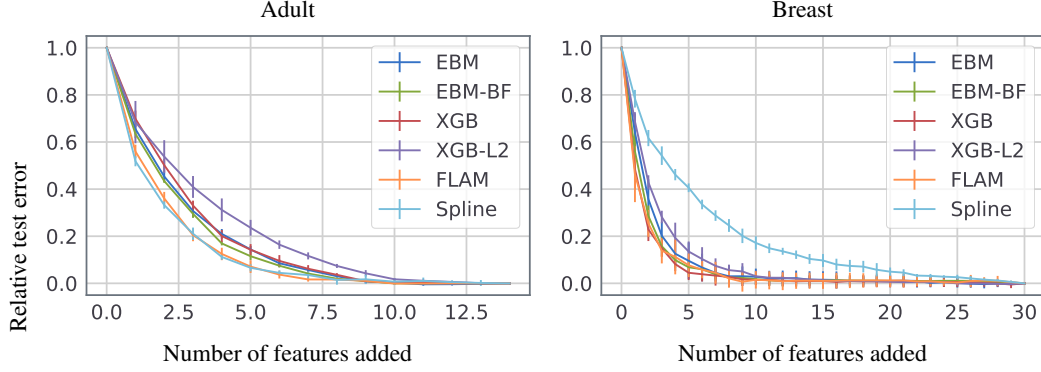


Figure 7: L2-ness plot. It shows how a model’s error (y-axis) decays as more features (x-axis) are given to the model in the Adult (left) and Breast (right) datasets. The steeper the model’s curve is, the fewer features it depends on.

that tends to underestimate instead of overestimating. On the other hand, Spline is the best at not underestimating the error but makes more overestimation error, probably due to its overshooting behaviors in the low-sample regions.

Table 9: The worst overestimation score among different generators.

	EBM	EBM-BF	XGB	FLAM	Spline	LR	iLR	mLR
Breast	0.000	0.774	0.284	0.000	0.787	0.497	0.000	0.823
Churn	0.448	0.655	0.492	0.722	0.000	0.000	0.483	0.000
Heart	0.808	0.934	0.684	0.840	0.969	0.858	0.911	0.000
MIMIC-II	0.723	0.849	0.792	0.708	0.553	0.000	0.102	0.000
MIMIC-III	0.748	1.000	0.806	0.794	0.202	0.315	0.097	0.000
Pneumonia	0.616	1.000	0.751	0.856	0.000	0.138	0.383	0.286
Average	0.557	0.869	0.635	0.653	0.419	0.301	0.329	0.185

Table 10: The worst underestimation score among different generators.

	EBM	EBM-BF	XGB	FLAM	Spline	LR	iLR	mLR
Breast	0.678	0.000	0.644	0.275	0.144	0.252	0.358	0.000
Churn	0.163	0.000	0.145	0.194	0.218	0.257	0.161	0.132
Heart	0.582	0.000	0.825	0.371	0.397	0.036	0.126	0.134
MIMIC-II	0.517	0.239	0.695	0.564	0.811	0.000	0.000	0.018
MIMIC-III	0.197	0.000	0.420	0.448	0.881	0.352	0.000	0.120
Pneumonia	0.328	0.000	0.418	0.418	1.000	0.622	0.379	0.295
Average	0.411	0.040	0.524	0.378	0.575	0.253	0.171	0.117

B.4 Full table of test AUCs on real data with standard deviation

We show the mean and standard deviation of test AUCs for all GAMs in Table 11.

B.5 Additional shape graphs

We qualitatively show the shape plots of 5 main GAMs trained on other datasets (MIMIC-II, Churning, Heart, Adult, and Breast) from Figure 8 to Figure 13.

Table 11: Test set AUCs (with std) across 10 different datasets. Best number in each row in **bold**.

	GAM					
	EBM	EBM-BF	XGB	XGB-L2	FLAM	Spline
Adult	0.930 ± 0.005	0.928 ± 0.005	0.928 ± 0.006	0.917 ± 0.006	0.925 ± 0.006	0.920 ± 0.006
Breast	0.997 ± 0.005	0.995 ± 0.005	0.997 ± 0.005	0.997 ± 0.005	0.998 ± 0.003	0.989 ± 0.008
Churn	0.844 ± 0.007	0.840 ± 0.009	0.843 ± 0.007	0.843 ± 0.007	0.842 ± 0.007	0.844 ± 0.008
COMPAS	0.743 ± 0.014	0.745 ± 0.017	0.745 ± 0.015	0.743 ± 0.015	0.742 ± 0.017	0.743 ± 0.015
Credit	0.980 ± 0.005	0.973 ± 0.013	0.980 ± 0.006	0.981 ± 0.006	0.969 ± 0.004	0.982 ± 0.007
Heart	0.855 ± 0.069	0.838 ± 0.060	0.853 ± 0.063	0.858 ± 0.070	0.856 ± 0.067	0.867 ± 0.063
MIMIC-II	0.834 ± 0.009	0.833 ± 0.008	0.835 ± 0.010	0.834 ± 0.009	0.834 ± 0.010	0.828 ± 0.008
MIMIC-III	0.812 ± 0.004	0.807 ± 0.007	0.815 ± 0.005	0.815 ± 0.005	0.812 ± 0.004	0.814 ± 0.004
Pneumonia	0.853 ± 0.006	0.847 ± 0.007	0.850 ± 0.008	0.850 ± 0.006	0.853 ± 0.009	0.852 ± 0.006
Support2	0.813 ± 0.010	0.812 ± 0.010	0.814 ± 0.011	0.812 ± 0.010	0.812 ± 0.011	0.812 ± 0.011
Average	0.866	0.862	0.866	0.865	0.864	0.865
Rank	3.70	6.70	3.40	4.90	5.05	4.60
Score	0.893	0.781	0.873	0.818	0.836	0.810
	GAM			Full		
	iLR	LR	mLR	RF	XGB-d3	
Adult	0.927 ± 0.005	0.909 ± 0.006	0.925 ± 0.004	0.912 ± 0.005	0.930 ± 0.006	
Breast	0.981 ± 0.005	0.997 ± 0.004	0.985 ± 0.005	0.993 ± 0.011	0.993 ± 0.011	
Churn	0.834 ± 0.010	0.843 ± 0.007	0.827 ± 0.010	0.821 ± 0.006	0.843 ± 0.007	
COMPAS	0.735 ± 0.013	0.727 ± 0.010	0.722 ± 0.013	0.674 ± 0.012	0.745 ± 0.015	
Credit	0.956 ± 0.006	0.964 ± 0.011	0.940 ± 0.014	0.962 ± 0.015	0.973 ± 0.007	
Heart	0.859 ± 0.063	0.869 ± 0.058	0.744 ± 0.053	0.854 ± 0.065	0.843 ± 0.046	
MIMIC-II	0.811 ± 0.010	0.793 ± 0.008	0.816 ± 0.007	0.860 ± 0.006	0.847 ± 0.007	
MIMIC-III	0.774 ± 0.010	0.785 ± 0.005	0.776 ± 0.003	0.807 ± 0.008	0.820 ± 0.007	
Pneumonia	0.843 ± 0.010	0.837 ± 0.006	0.845 ± 0.007	0.845 ± 0.005	0.848 ± 0.008	
Support2	0.800 ± 0.012	0.803 ± 0.007	0.772 ± 0.009	0.824 ± 0.010	0.820 ± 0.014	
Average	0.852	0.853	0.835	0.855	0.866	
Rank	8.70	7.75	9.70	7.40	4.10	
Score	0.474	0.507	0.285	0.543	0.865	

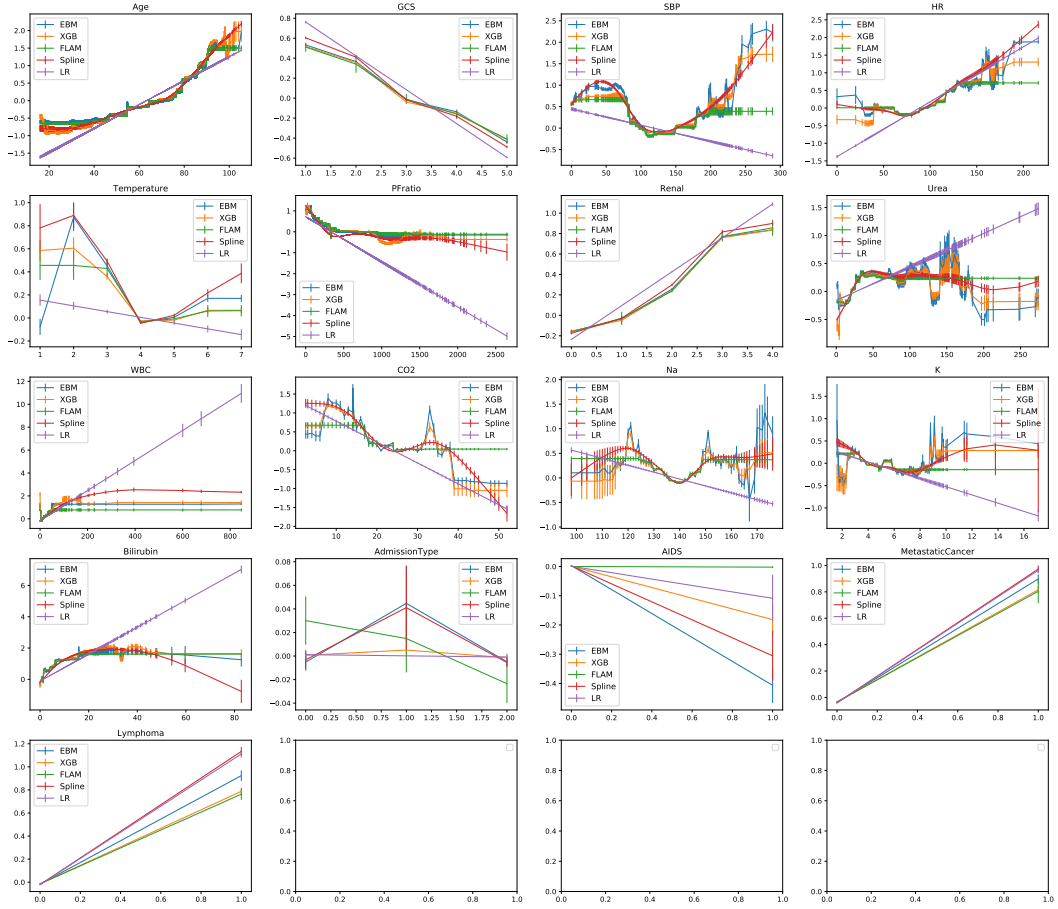


Figure 8: The shape plots of 5 main GAM models trained on the MIMIC-II dataset.

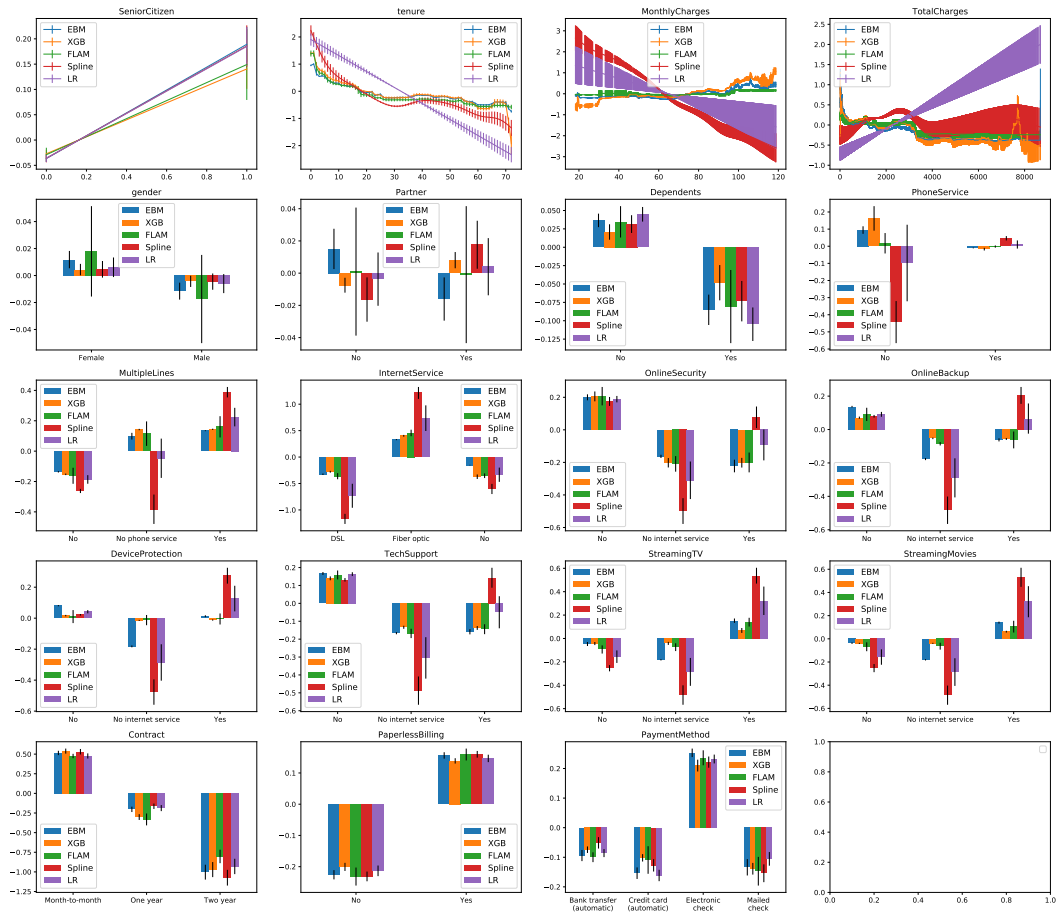


Figure 9: The shape plots of 5 main GAM models trained on the subscription Churning dataset.

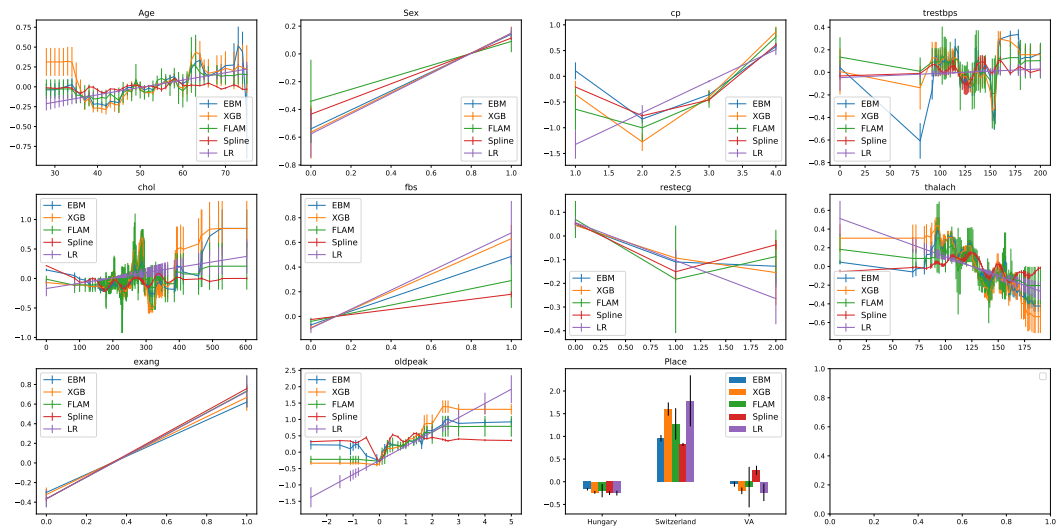


Figure 10: The shape plots of 5 main GAM models trained on the Heart disease UCI dataset.

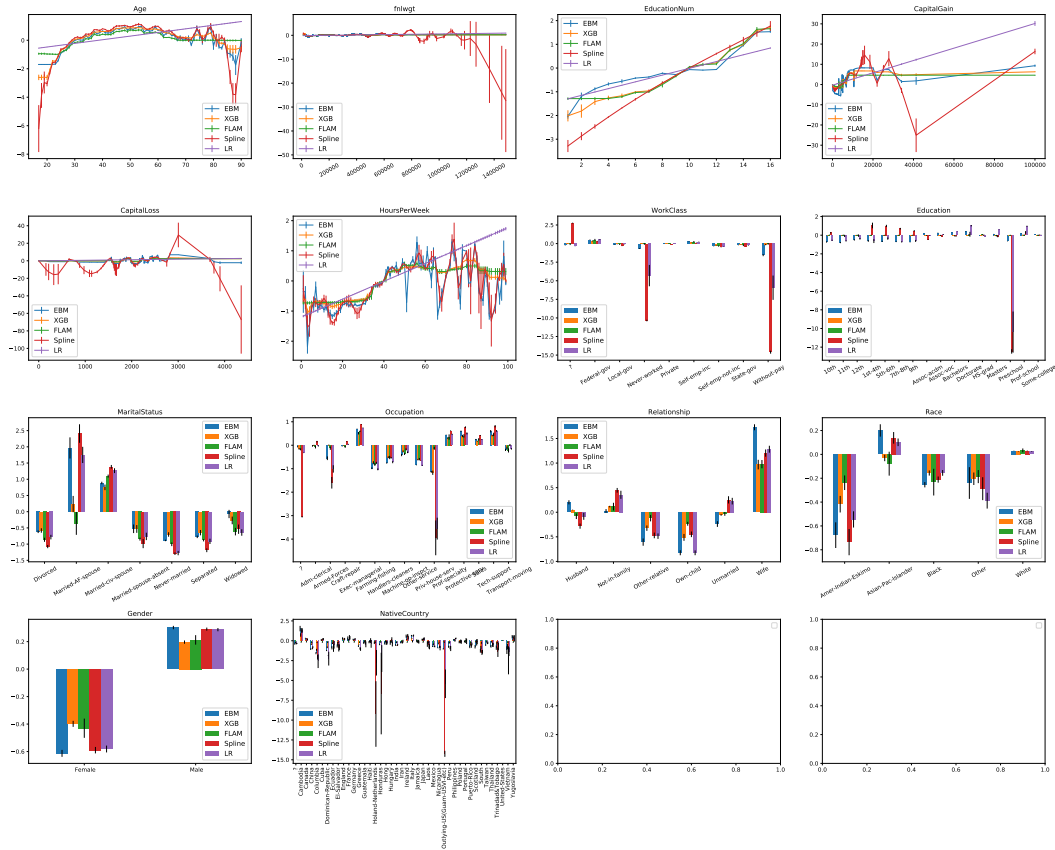


Figure 11: The shape plots of 5 main GAM models trained on the Adult Income prediction datasets.

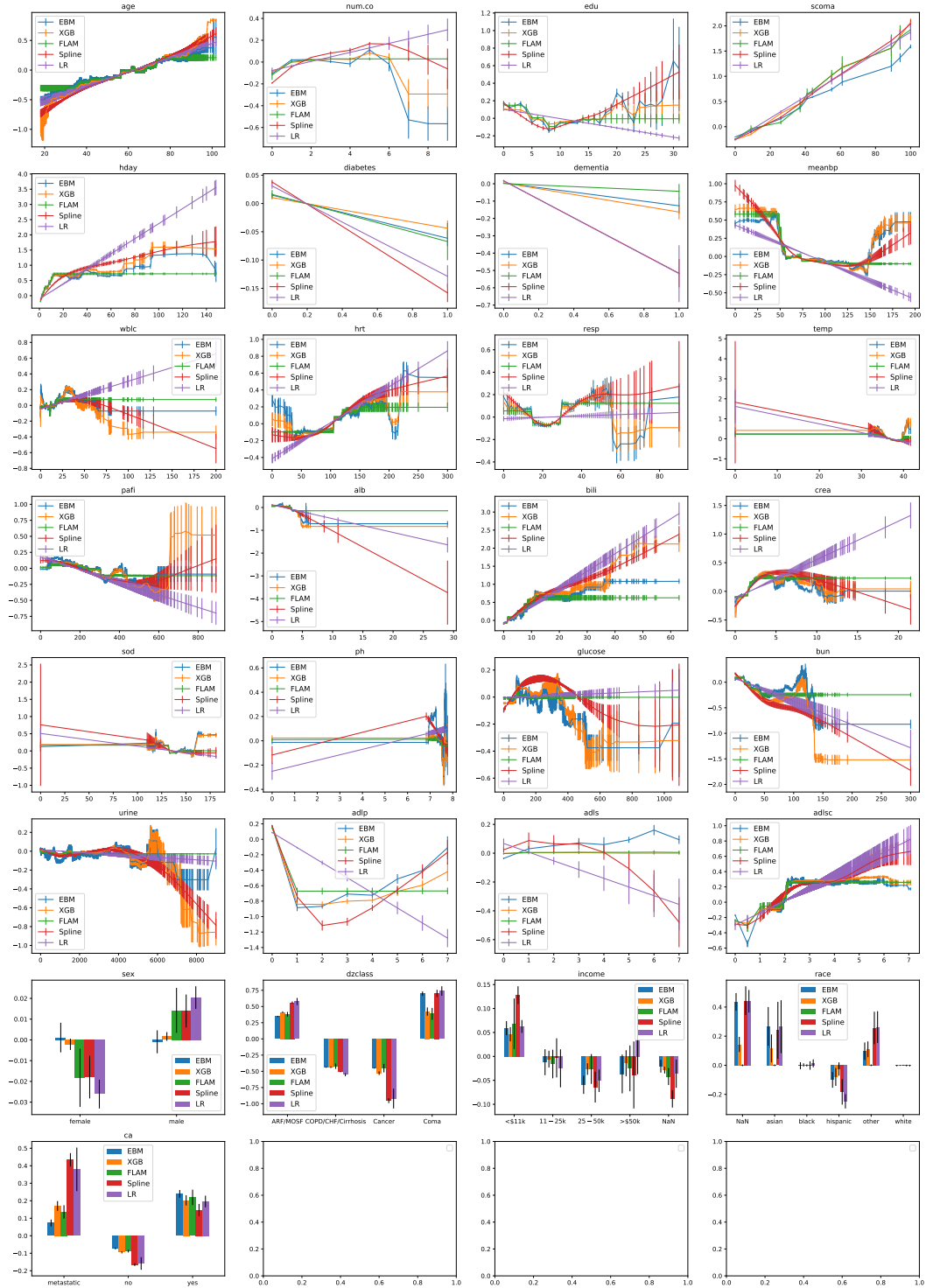


Figure 12: The shape plots of 5 main GAM models trained on the Support2 dataset to predict hospital mortality.

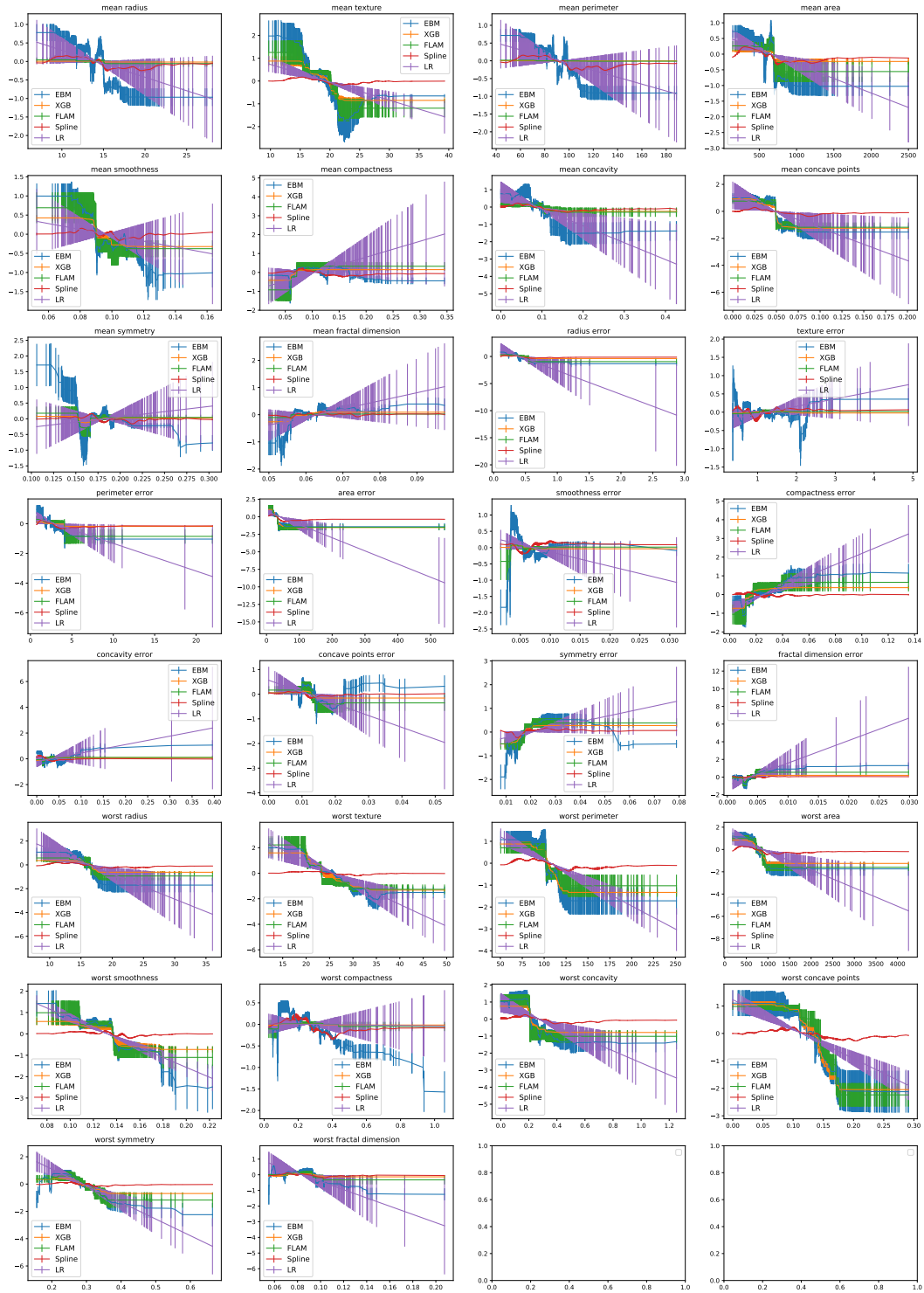


Figure 13: The shape plots of 5 main GAM models trained on the Breast Cancer UCI dataset.